Synthesis of $(Ba_{1-x}Sr_x)(Ti_{0.5}Zr_{0.5})O_3$ ceramics and effect of Sr content on room temperature dielectric properties.

J. Bera*, Department of Ceramic Engineering
S.K. Rout, Department of Physics
National Institute of Technology, Rourkela-769 008, INDIA

Abstract

The compositions in the system $(Ba_{1-x}Sr_x)(Ti_{0.5}Zr_{0.5})O_3$ with different Sr (x) content, were synthesized through solid oxide reaction route. The phase formation behaviors in the system were investigated by XRD. The room temperature dielectric properties of the compositions were investigated in the frequency range 10Hz to 13 MHz. The solid solution system $Ba_{1-x}Sr_xTi_{0.5}Zr_{0.5}O_3$ remains as cubic perovskite up to x<0.6 and transforms into the tetragonal structure above x>0.6. Composition with x=0.6 contains a mixture of cubic and tetragonal phases with broadened diffraction pattern. It is observed that the increasing of Sr substitution results in the decreasing of bulk density, average grain size and dielectric constants etc. in the composition system. The AC dielectric conductivity of the ceramics also decreases with the increase in Sr-substitution due to decrease in loss as well as grain size with that substitution.

Key wards: Electroceramics; Perovskites; Barium-strontium titanate-zirconate, Phase formation; Permittivity

---

1. Introduction

High permittivity $Ba(TiZr)O_3$ material is often used for dielectrics in commercial capacitor applications [1] and is highly promising material for dynamic random access memory (DRAM) [2], microelectromechanical system (MEMS) [3] applications due to its very stable, high insulating characteristic against voltage. $BaTiO_3$ (BT) is known to form complete solid solution with $BaZrO_3$ (BZ). It has been reported [1] that at ~15 atom % Zr substitution the three transition temperatures of $BaTiO_3$, rhombohedra to orthorhombic, orthorhombic to tetragonal and tetragonal to cubic, merge near room temperature and the doped material exhibits enhanced dielectric constant. With further increase in Zr contents beyond 15 atoms %, a diffuse dielectric anomaly in ceramic has been observed with the decrease in the transition temperature [4] and the

---
* Corresponding author. Tel.: +91 9437246159;
fax: +91 661 2462926.
E-mail: jbera@nitrkl.ac.in   (J. Bera).

material showed typical relaxor–like behavior in the range 25-42 atom % Zr substitution [5]. Most of the literature in the system $Ba(Ti_{1-x}Zr_x)O_3$ is restricted up to the value of x ~0.4 [2,3,6]. That is the reason, 50 atom% Zr substituted composition $Ba(Ti_{0.5}Zr_{0.5})O_3$ (BTZ) has been taken as a base material for the investigation of the effect of Sr substitution for Ba on its dielectric properties. It is well known that $SrTiO_3$ forms complete solid solution with $BaTiO_3$. That barium strontium titanate (BST) ceramics are also popular for DRAM applications [7]. The Ba/Sr titanate-zirconate ceramics (BSTZ) are reported to have improved tunability and low temperature coefficient of dielectric constant [8-10]. In the present investigation, the effect of Sr substitution for Ba on the phase formation behavior and room temperature dielectric properties of $(Ba_{1-x}Sr_x)(Ti_{0.5}Zr_{0.5})O_3$ ceramics were studied.

2. Experimental

The samples were prepared through solid state reaction route. The compositions with different values of x (=0.2, 0.4, 0.5, 0.6, 0.8, and 1.0) in $Ba_{1-x}Sr_xTi_{0.5}Zr_{0.5}O_3$ were synthesized from $BaCO_3$ (S.D. Fine Chem., Mumbai), $SrCO_3$ (S.D. Fine Chem., Mumbai), TiO_2 (E. Merck India Ltd.) and ZrO_2 (Loba Chem., Mumbai) raw powders. All the chemicals were having more than 99% purity. The raw powders were thoroughly mixed in agate mortar using IPA. The homogenous mixtures were calcined successively at: 1300^0C for 4h, 1400^0C for 4h and finally 1600^0C for 1h with intermediate mixing and grinding. The synthesized powders were characterized with respect to phase identification and lattice parameter measurements, using Cu-K_α XRD (PW-1830, Philips, Netherlands). For electrical property measurements, the disks were pressed uniaxially at 200 Mpa with 2wt% PVA added as binder. The pressed pellets were sintered at 1450^0C for 30 hrs. The bulk density and apparent porosity of sintered pellets were evaluated using Archimedes principle. The X-ray density was calculated as suggested by B.D. Cullity [11]. The microstructure of the sintered pellets were analyzed by optical microscope (Zeiss Axiotech Optical Microscope). Silver electrodes were printed on to the opposite disk faces and were sintered at 700^0C, 15 minutes. The room temperature dielectric measurements were carried out over 10Hz to 13MHz frequency range using HP-4192A LF Impedance Analyzer. The AC conductivity of the samples was calculated using capacitance and tanδ values.

3. Results and Discussion

Fig. 1 shows the room temperature XRD pattern of the $Ba_{1-x}Sr_xTi_{0.5}Zr_{0.5}O_3$ ceramics with different Sr (x) concentration. The XRD patterns were indexed and cell parameters were refined by using standard CCP-14 program "CHEKCELL" [12]. It is evident from the figure that all the peaks correspond to perovskite phase. The composition with x=0.0, i.e, $Ba(Ti_{0.5}Zr_{0.5})O_3$ was indexed in cubic system (space group Pm-3m) and the pattern was very similar to the standard PDF-2 card No. 36-0019 (for Cubic $BaTi_{0.75}Zr_{0.25}O_3$). It has been suggested that the solid solution $Ba(Ti_{1-x}Zr_x)O_3$ does not exist for x>0.42 [13]. However, in the present investigation the solid solution $Ba(Ti_{0.5}Zr_{0.5})O_3$ was found to exist as a single phase perovskite. The ceramic compositions were synthesized in the present study through successive calcinations and long time sintering etc. These processing may be responsible for the formation of a single phase solid solution of the same. With increase in Sr, the BSTZ system remains cubic upto 50 atom% substitution; only peaks were shifted towards higher angle yielding the decrease in lattice parameter due to the substitution of bigger Ba^{+2} (R=1.35 Å) by smaller Sr^{+2} (R = 1.13 Å) in the structure.
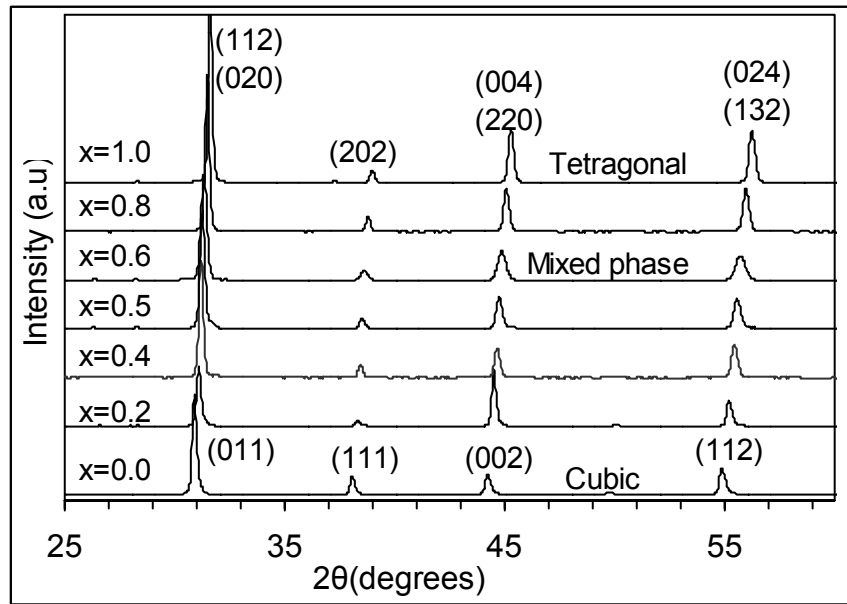

Fig.1. XRD pattern of $(Ba_{1-x}Sr_x)Ti_{0.5}Zr_{0.5}O_3$ ceramics with different Sr (x) content.

The lattice parameters of different compositions are shown in Table-1. The pattern of composition x=0.6 appears to contain both the cubic and tetragonal phases. Because, (a) both cubic and tetragonal indexing was possible on the pattern (the lattice parameters for both the

indexing are shown in Table 1) and (b) it shows relatively higher FWHM (Table 1) of its diffraction peaks. However, the patterns of x=0.8 and 1.0, were indexed in tetragonal system. The composition, x=1.0, i.e, $Sr(Ti_{0.5}Zr_{0.5})O_3$ (STZ) is reported to be tetragonal [14,15] with space group I4/mcm. So upon Sr substitution in BTZ, the structure changes from Pm-3m cubic (Z=1) to I4/mcm tetragonal (Z=4) above x>0.6. It is well known that the lower symmetry structures are also characterized by the splitting of reflections. Such peak splitting in the present tetragonal structure can be observed using higher resolution synchrotron diffraction measurements [14]. The 100% relative intensity peak widths of all the compositions were compared (Table-1). Compositions with x=0.6 shows highest FWHM among all mainly due to the presence of both cubic and tetragonal phases in it. The composition x=0.5 shows slightly higher FWHM, may be due to the presence of 50:50 ratio of $Ba(Ti_{0.5}Zr_{0.5})O_3$ and $Sr(Ti_{0.5}Zr_{0.5})O_3$ in the solid solution.

Table 1
Crystal symmetry, lattice parameter, FWHM (100% relative intensity peak), X-ray density, bulk density and apparent porosity of the $(Ba_{1-x}Sr_x)Ti_{0.5}Zr_{0.5}O_3$ compositions with different Sr (x) content.

x	Symmetry	Lattice parameter(Å)	FWHM of $I_{100\%}$ peak	X-ray Density (gm/cc)	Bulk Density (gm/cc)	Apparent Porosity (%)
0	Cubic	a_0=4.101(02)	0.131	6.14	5.75	2.0
0.2	Cubic	a_0=4.078(07)	0.116	5.99	5.65	2.5
0.4	Cubic	a_0=4.065(02)	0.149	5.81	5.35	3.1
0.5	Cubic	a_0=4.057(07)	0.167	5.72	5.20	3.4
0.6	Cubic + Tetragonal	a_0=4.042(06) and a_0=5.717(15) c_0=8.104(21)	0.263	5.66 5.64	4.92	4.2
0.8	Tetragonal	a_0=5.694(06) c_0=8.064(04)	0.140	5.46	4.78	4.7
1.0	Tetragonal	a_0=5.671(03) c_0=8.023(06)	0.138	5.38	4.44	7.2

Fig. 2 shows the variation of bulk density and percentage apparent porosity with different Sr (x) concentration in $Ba_{1-x}Sr_x(Ti_{0.5}Zr_{0.5})O_3$ ceramics with same sintering conditions for all compositions. The values of these parameters are also shown in the Table 1. The calculated X-ray density was found to decrease with Sr substitution. As expected, the bulk density also decreases with the increase in Sr substitution. The apparent porosity was found to increase with the Sr substitution. This indicates that the $Ba_{1-x}Sr_x(Ti_{0.5}Zr_{0.5})O_3$ ceramics with x=0.0 composition ($BaTi_{0.5}Zr_{0.5}O_3$) is easy to sinter than x=1.0 composition i.e. $SrTi_{0.5}Zr_{0.5}O_3$ (STZ) ceramics. The better sintering behavior of BTZ may also be reveled from its bigger grain size (Fig.3) in the sintered ceramics. The average grain size of BTZ and STZ ceramics are 17.5 and 2.2 micron respectively (Fig.3). The average grain sizes of the compositions in between these two end members were found to decrease progressively with increase in Sr substitution. So, it can be expected that high Sr-containing compositions require increased sintering temperature or time to achieve higher density.
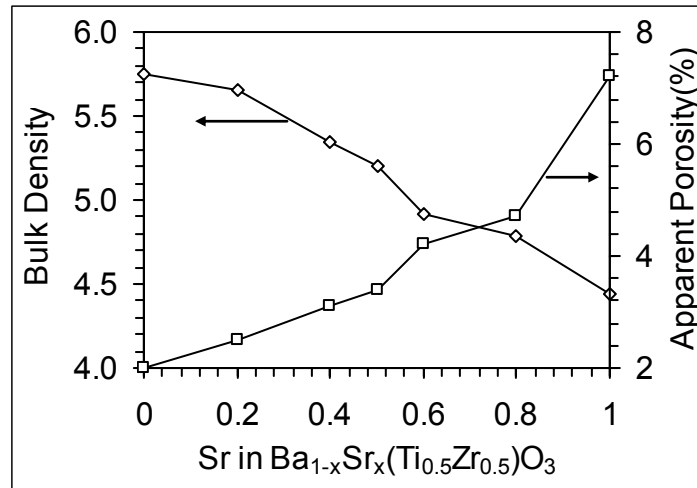

Fig. 2. Effects of Sr (x) content on bulk density and apparent porosity of $Ba_{1-x}Sr_x(Ti_{0.5}Zr_{0.5})O_3$ ceramics.
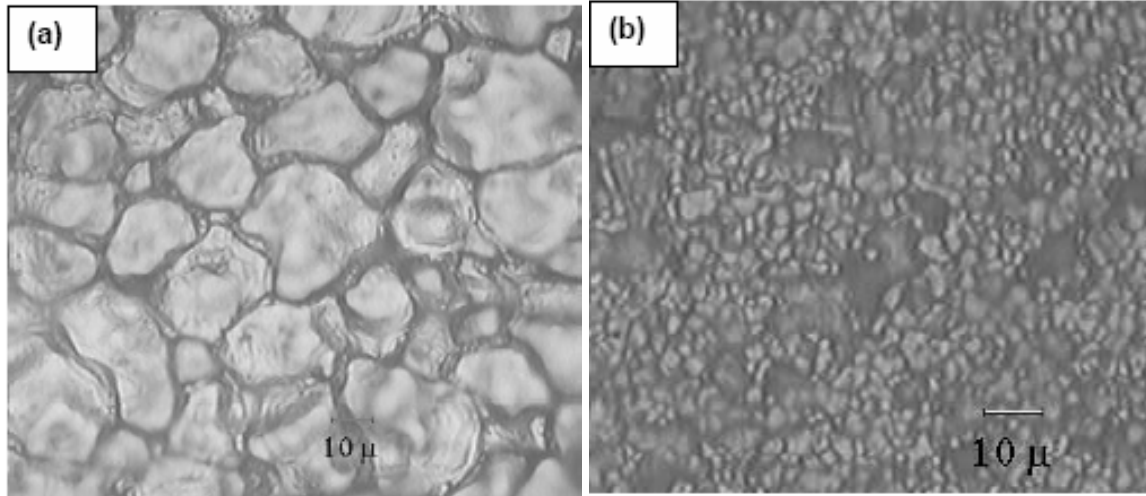
Fig.3 Microstructure of sintered $Ba_{1-x}Sr_xTi_{0.5}Zr_{0.5}O_3$ ceramics with (a) x=0.0 and (b) x=1.0.

Fig. 4 shows the frequency dependency dielectric constant of $Ba_{1-x}Sr_xTi_{0.5}Zr_{0.5}O_3$ compositions. The BSTZ composition with x=0.0, shows the highest dielectric constant. The dielectric constant decreases with Sr substitution yielding the lowest dielectric constant in x=1.0 composition. However, the compositions x=1.0 and x=0.8 should show slightly higher dielectric constant due to their tetragonal (ferroelectric) structure. The lower permittivity of the two compositions may be attributed to their lower density and lower grain size in the sintered dielectrics. The dielectric constant of all the compositions was very stable in the frequency range 1 kHz to about 7 MHz. In general dielectric constant decreases with the increase in Sr substitution due to; (i) the decrease in concentration of high permittivity material BTZ and (ii) due to the decrease in polarizability of the atoms in the structure. When a lower radius Sr replaces higher radius Ba in the structure, there is a decrease in lattice parameter yielding the lowering of dipole moment in cubic perovskite.
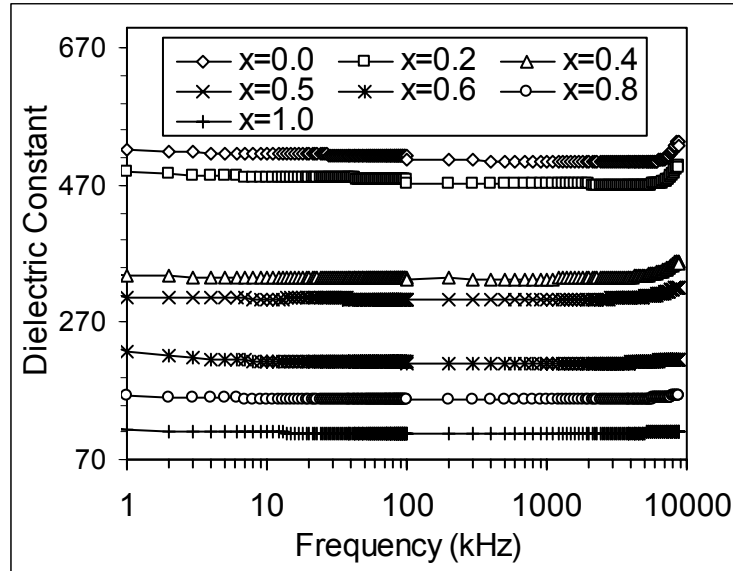
Fig. 4 Frequency dependency of permittivity of different $Ba_{1-x}Sr_x(Ti_{0.5}Zr_{0.5})O_3$ compositions.

Fig. 5 shows the frequency dependency of the dielectric loss of the samples. The loss was found to decrease nominally with the increase in Sr substitution. This may be primarily attributed to the decrease in dielectric constant with Sr substitution. In general high permittivity materials possess higher losses. Other reason may be the effect of increased Sr-content. It is known that Q-factor of BST ceramics increases with the increase in Sr-content [16]. The loss is stable as well as fairly low (<0.6%) for all the compositions in the frequency range 100 KHz to about 5MHz. Below 100 kHz, the loss was progressively higher with the decrease in frequency mainly due to the space charge polarization phenomena. The dispersion of loss at higher frequency (>~5 MHz) is due to some extrinsic loss phenomena [17]. This is to note that the frequency dependency of permittivity shows almost stable behavior and dielectric losses are very low for all compositions in bulk ceramics in the frequency range 100 kHz to 5 MHz. The materials are suitable for low loss application in the said frequency range.
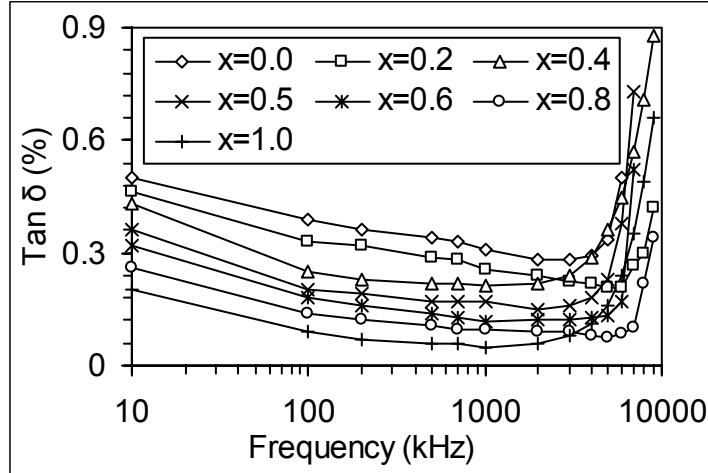
Fig. 5 Frequency dependency of dielectric loss of different $Ba_{1-x}Sr_x(Ti_{0.5}Zr_{0.5})O_3$ compositions.

For through analysis of the electrical properties, conductivity (σ) of the samples were calculated using the formula $\sigma = 2\pi fd\ C\ \tan\delta/A$. Where; f is the operating frequency, d is the thickness of the dielectrics, $\tan\delta$ is the dielectric loss, C is the capacitance and A is the area of the electrode. The variation of ac conductivity with Sr content in the composition system is plotted in the Fig. 5. The conductivity was found to decrease with increase in Sr concentration as well as increase in frequency. The decrease in conductivity may be primarily due to the decrease in $\tan\delta$ loss with Sr substitution as stated earlier. Also that decrease may be partly due to the decrease in grain size and hence increase in grain boundary areas/resistance with Sr substitution. Grain boundary areas are highly resistive in oxide ceramics. Smaller grain sized ceramics has larger grain boundary areas and hence higher resistivity than bigger grain sized ceramics.
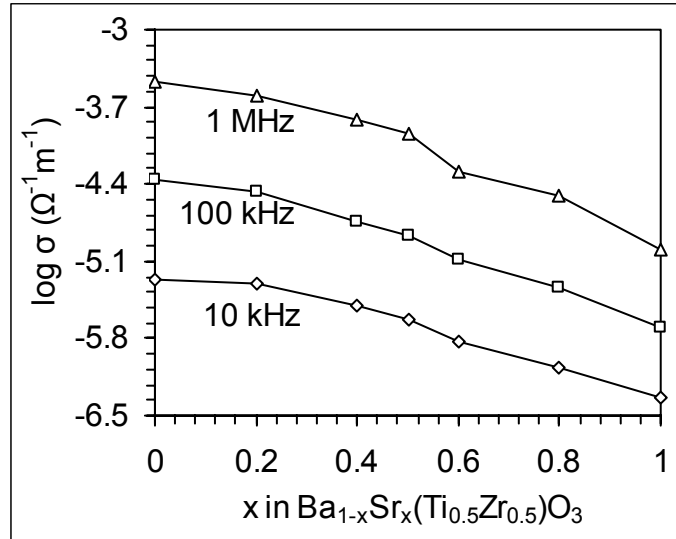
Fig. 6 Variation of AC conductivity with Sr (x) content in $Ba_{1-x}Sr_x(Ti_{0.5}Zr_{0.5})O_3$ ceramics.

4. Conclusions

It may be concluded from the present investigation that:

1. The solid solution system $Ba_{1-x}Sr_x(Ti_{0.5}Zr_{0.5})O_3$ remains cubic up to x<0.6 and becomes tetragonal in the range x >0.6 to x=1.0.
2. Composition with x=0.6 contains both the cubic and tetragonal phases.
3. The compositions show decreased densification and grain growth with the increase in Sr substitution.
4. Composition with x=0.0 (BTZ) shows highest permittivity in the system. The permittivity and dielectric loss decrease with the increase in Sr substitution.
5. The permittivity and loss are found to be stable and loss is less than 0.6 % in the frequency range 100 kHz to about 5 MHz for all the compositions.
6. AC conductivity in the ceramics decreases with Sr-substitution due to the decrease in loss as well as grain size.

References

[1]   D. Henning, A. Schnell, G Simon, J Am. Ceram Soc, 65, 539 (1982).

[2]   T. B. Wu, C. M. Wu and M. L. Chen, Appl Phys Lett, 69 (18), 2659 (1996).

[3]   A. Dixit, S.B. Majumder, R.S. Katiyar, A.S. Bhalla, Appl. Phys. Lett, 82, 2679 (2003).

[4]   Z .Yu, R. Guo, A.S. Bhalla, J.appl. Phys, 88, 410 (2000).

[5]   Z. Yu, C. Ang, R. Guo, A.S. Bhalla, Appl. Phys. Lett, 81, 1285 (2002).

[6]   C. Hofer, R. Meyer, U. Bottger, R. Waser, J Euro. Cera. Soc., 24, 1473 (2004).

[7]   K. Abe, S. Komatsu, J.appl. Phys, 77, 6461 (1995).

[8]   S.G. Lu, X. H. Zhu, C. L. Mak, K. H. Wong, H. L. W. Chan, C. L. Choy, Appl Phys Lett. 82, 2877 (2003).

[9]   X. H. Zhu, N. Chong, H. Lai-Wah Chan, C. L. Mak, K. H. Wong, Z.G. Liu, N. B. Ming, Appl Phys Lett 80, 3376 (2002).

[10] C. Wang, B. L. Cheng, S. Y. wang, H. B. Lu, Y. L. Zhou, Z. H. Chen, G. Z. Yang, Appl Phys Lett, 84 (5), 765 (2004).

[11] B. D. Cullity, "Elements of x-ray diffraction", 2nd Edition, Addison- Wesley Publishing company, Inc. (1978).

[12] http:/www.ccp14.ac.uk/tutorial/lmgp/

[13] Ph. Sciau, G. Calvarin, J. Ravez, Solid State Comm., 113, 77-82 (2000).

[14] T.K.Y. Wong, B. J. Kennedy, C. J. Howard, B. A. Hunter, T. Vogt, J Solid State Chemistry, 156, 255 (2001).

[15] J.Bera, S.K.Rout, Mat. Res. Bull., 40, 1187-1193(2005).

[16] A. Ioachim, M.I. Toacsan, M.G. Banciu, L. Nedelcu, C. Plapcianu, H. Alexandru, C. Berbecaru, D. Ghetu, G. Stoica, R. Ramer, J. Optoelectron. Adv. Mater. 5 (2003) 1389.

[17] L.I. Maissel, R. Glang, Handbook of Thin Film Technology, McGraw-Hill, New York, 1970 (Chapter 16).